

## References

- 1) D. Pooley, Proc. Phys. Soc. **87** (1966) 245;
- 2) H. N. Hersch, Phys. Rev. **148** (1966) 928;
- 3) J. H. Crawford, Advances in Physics **17** (1968) 93;
- 4) P. D. Townsend and D. J. Elliott, Physics Letters **28A** (1969) 587;
- 5) M. Prutton, private communication;
- 6) A. D. G. Stewart and M. W. Thompson, J. Materials Science **4** (1969) 56.

### 2.13 Oxidation patterns due to bombardment under variable incidence of copper monocrystals by oxygen ions

M. MEYER and C. MARELLE, *Laboratoire Rayons, C.N.R.S. Bellevue, France.*  
 P. HAYMANN, *Faculté des Sciences de Rouen. Rouen X, France*

### 2.14 Microtopography of metal surfaces eroded by ion bombardment

I. A. TEODORESCU, *Institute for Atomic Physics, Bucharest, Romania*

### 2.15 On the origin of surface topography on ion bombarded metal samples

N. HERMANNE and A. ART, *Physique des Surfaces, Faculté des Sciences, Université libre de Bruxelles, Brussels, Belgium*

Our replica and transmission EM studies on ion (Argon) bombarded Cu samples (dose:  $10^{16}$  ions/cm<sup>2</sup>)<sup>1)</sup> and the observations of several other authors<sup>2)</sup> enables us to propose a model for the formation of the surface structure which appears on the surface of ion-bombarded metal samples.

The fact that our experiments on bombarded bulk material and bombarded thin foils (electropolished before bombardment) give exactly the same results as far as relief structure is concerned, proves firstly that the obtained features are independent of the preparation methods<sup>1)</sup> before bombardment of both type of samples, thus excluding electrochemical etching and thermal effects. Secondly that the mechanism must be one compatible with bulk as well as thin material, thus concerns a number of layers not exceeding a thickness of the thin films ( $\approx 150$  atomic layers).

On the other hand, due to the values of the sputtering yield<sup>3)</sup> that correspond to the crystal orientation of the grains on which this surface structure

is observed, the surface of these grains regresses at a high rate (for example several layers per sec. on a  $\langle 100 \rangle$  grain). It is thus impossible that the origin of this organized topography could be due to surface effects such as surface diffusion, direct extraction of surface atoms by the incident ions or any other mechanism involving a few surface layers only. The origin of the formation of the relief structure is thus related to phenomena acting deeper inside the crystal. This is confirmed by our observations.

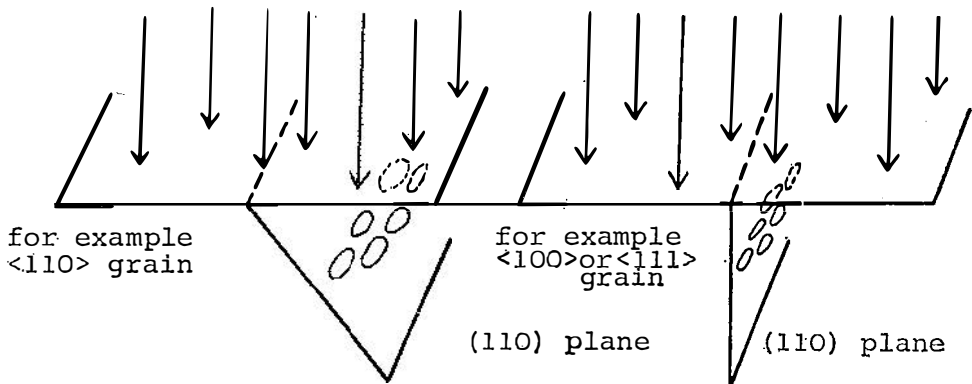
Indeed, apart from the relief structure, we also observed after ion bombardment the presence in the foils of different types of dislocation-networks. One of these networks appears to have the same spacing (2000 Å) as the surface relief structure on a same grain and on the other hand they have the same dependence upon the orientation of the considered grain and certain directions in the surface. They are indeed<sup>1)</sup> aligned along the intersections of the (110) planes with the surface of the foil. These planes intersect the surface of the different grains along different directions.

{E. g., a) grains  $\langle 111 \rangle$  are intersected along  $\langle 112 \rangle$  directions (there are 3 of these forming angles of  $60^\circ$  between them, b) grains  $\langle 100 \rangle$  intersected along  $\langle 110 \rangle$  directions (two of them forming angles of  $90^\circ$  between them), c) grains  $\langle 110 \rangle$  are intersected along  $\langle 110 \rangle$  directions (only one).}

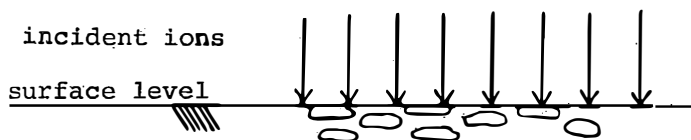
Our qualitative model to explain the origin of surface topography after ion bombardment is based as follows on the observation of this complete similarity between the arrangement of dislocations and that of surface relief.

The defects induced during collision cascades of the incoming ions, are point defects (vacancies or interstitials<sup>4)</sup>) located under the foil surface according to the damage depth distribution.

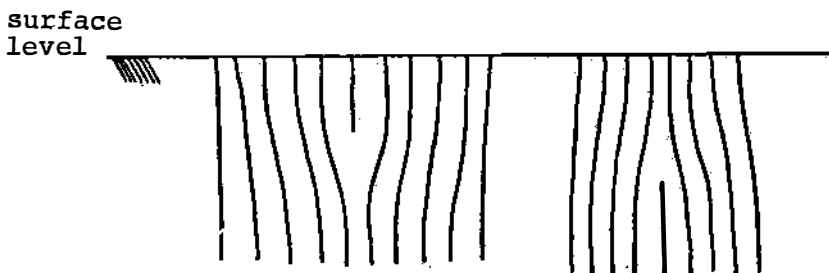
These defects migrate and, if their concentration is high, they form clusters, frequently observed by transmission E. M. owing to their black and white contrast<sup>5)</sup> (Fig. 1). These clusters become small dislocation loops, which grow by „swallowing up“ freshly induced defects. These loops lie in the (110) planes, which are perpendicular or not to the foil surface depending of the considered crystal orientation.



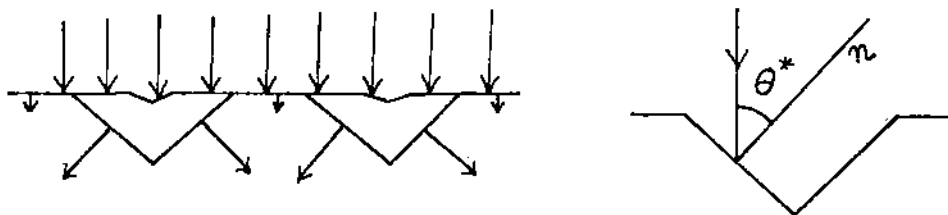
The surface, during the going on of the bombardment recedes by sputtering and will reach the level of the loops. Cutten by the surface these loops open (Fig. 2).



The neighbouring parts of the open loops, which lie in the same family of (110) planes, will interact, due to their opposite Burgers vector sign, to form long dislocation segments (Fig. 3), which lie very near the surface (black and white contrast<sup>6</sup>). These dislocation lines now will either attract to form longer dislocations, either repel mutually to reach a configuration of parallel lines, depending on their initial relative position. This network can extend over

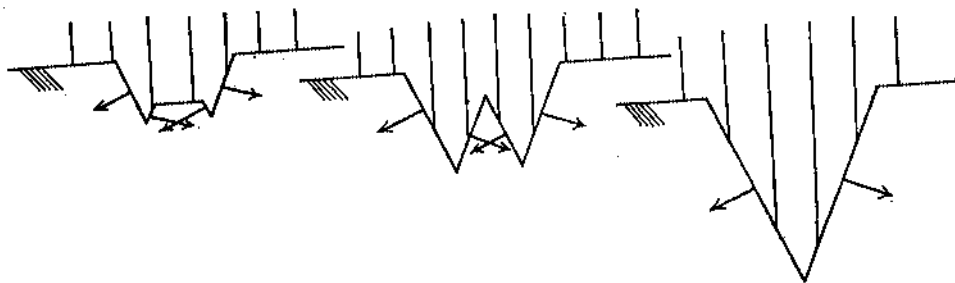


the whole width of the grain (Fig. 4). These dislocations are entire edge dislocations formed either by the presence of an extraplane (in the case the induced point defects were interstitials), either by lack of one plane (in the case the induced point defects were vacancies).



For the incoming ions their presence under the surface is a cause for dechanneling (7). The sputtering yield thus locally increases just above these dislocations, i. e. along the intersection of the (110) planes and the foil surface.

Consequently small ribs (Fig. 5) parallel to the dislocation lines appear in the surface which grow out to form an alignment of grooves by a mechanism similar to the one described by Stewart-Thompson to explain the formation of cones on polycrystalline surfaces during ion bombardment<sup>8)</sup>. Indeed, the walls of the grooves have an inclination with respect to the direction of the incident ions corresponding to a higher sputtering yield than the undisturbed parts of the surface and thus regress quicker during the going on of the bombardment.



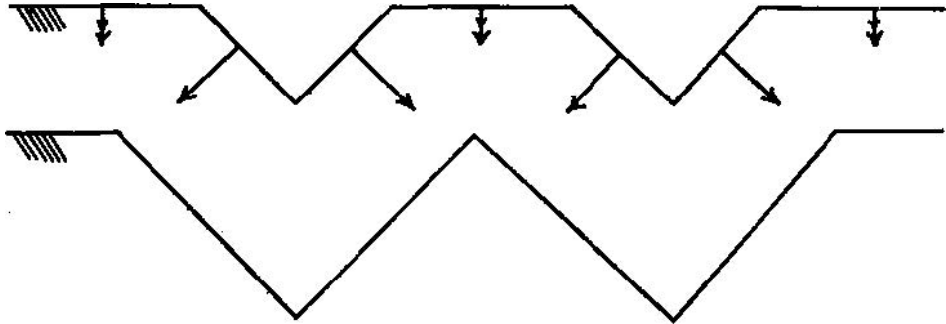
This variation in sputtering yield originates in a double effect. Firstly there is a variation of angle of incidence (angle between the surface normal and the direction of the incident beam) and secondly the crystal orientation of the surface, locally seen by the incoming ions, is not the same for the original surface as for the walls of the grooves. As this second variation is always one leading to orientations of higher  $hkl$  indices, this will thus correspond to an increase of sputtering yield. Which of both effects is predominant is not yet known.

The inclination of the walls increases until an angle  $\theta^*$  between the surface normal and incident beam is reached which corresponds to a maximum in sputtering yield.

In an intermediate stage the grooves could take the form of W. This stage could be the origin of formation of cones in the bottom of craters if an impurity was present on the surface before the beginning of the bombardment<sup>9)</sup>. The grooves become deeper due to the continuous regress of the surface and will finally join each other to reach the roof structure configuration (Fig. 7).

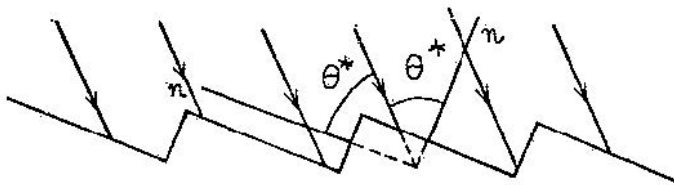
When considering the angle between the local surface normal of the roofstructure and the direction of ion incidence one has to remember that we are concerned with single crystals. As we start from the rather flat walls of the initial little grooves,  $\theta^*$  will correspond to the first maximum encountered when starting from the  $\theta = 0^\circ$  to higher  $\theta$  values in the curve of the variation of sputtering yield with the angle between incident beam and surface normal.

The resulting configuration of relief topography on each grain depends of the crystal orientation of the concerned grain. On those grains where different systems can develop, the resulting aspect is due to the intersection of this different systems of roofs.



As the dislocations are formed in the  $(110)$  planes and as the grooves appear along the intersection of these planes with the surface, the number of roof systems that can develop is thus equal to the number of families of  $(110)$  planes cutting the surface of the considered grain.

This explains how are formed for example triangular craters on the  $\langle 111 \rangle$  grains (3 systems intersecting) (Fig. 6) and square shaped craters on the  $\langle 100 \rangle$  grains (2 systems intersecting) (Fig. 7), but only one system of roof structure around the  $\langle 110 \rangle$  pole (Fig. 8).



For normal incidence both facets of the roof structure will develop symmetrically, even on those grains where the  $(110)$  planes do not intersect the foil surface perpendicularly.

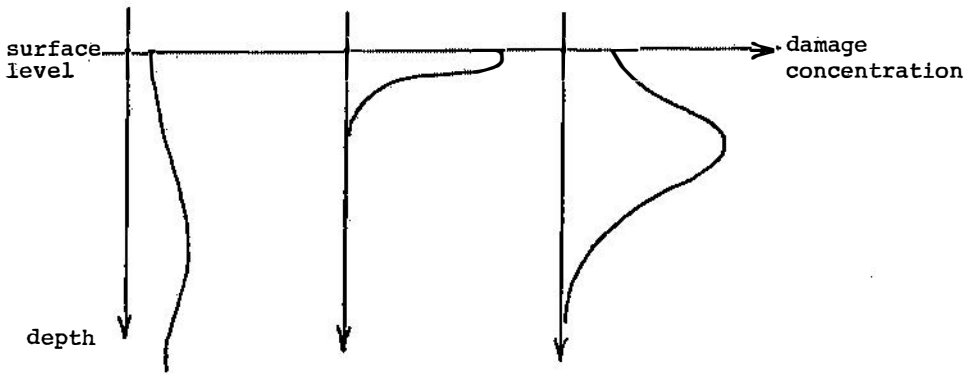
For non-normal incidence the roof structure will not more be symmetrical. Indeed each facet will develop to reach the same angle with respect to the beam, which corresponds to the same maximum in sputtering yield.

It is the previous discribed microtopography which causes the „milky appearance“ by Rayleigh diffusion of the incident light of the optical microscope ( $\lambda = 5000 \text{ \AA}$ , distance  $d = 2000 \text{ \AA}$ ).

When observing the bombarded drop shaped monocrystal (normal incidence) as well as the bombarded polycrystalline thin foils, the question arises why the relief structure does not develop during the ion bombardment on all possible grains, independent of the crystal orientation.

A necessary condition for starting the mechanism is a minimum concentration of point-defects induced at certain depth under the surface. The depth and spread of the damage due to the bombardment depends upon the penetration of the incoming ions, which itself depends of the transparency of the crystal for each crystal orientation.

Three types of crystal orientations which behave differently have to be distinguished: (see figures below)

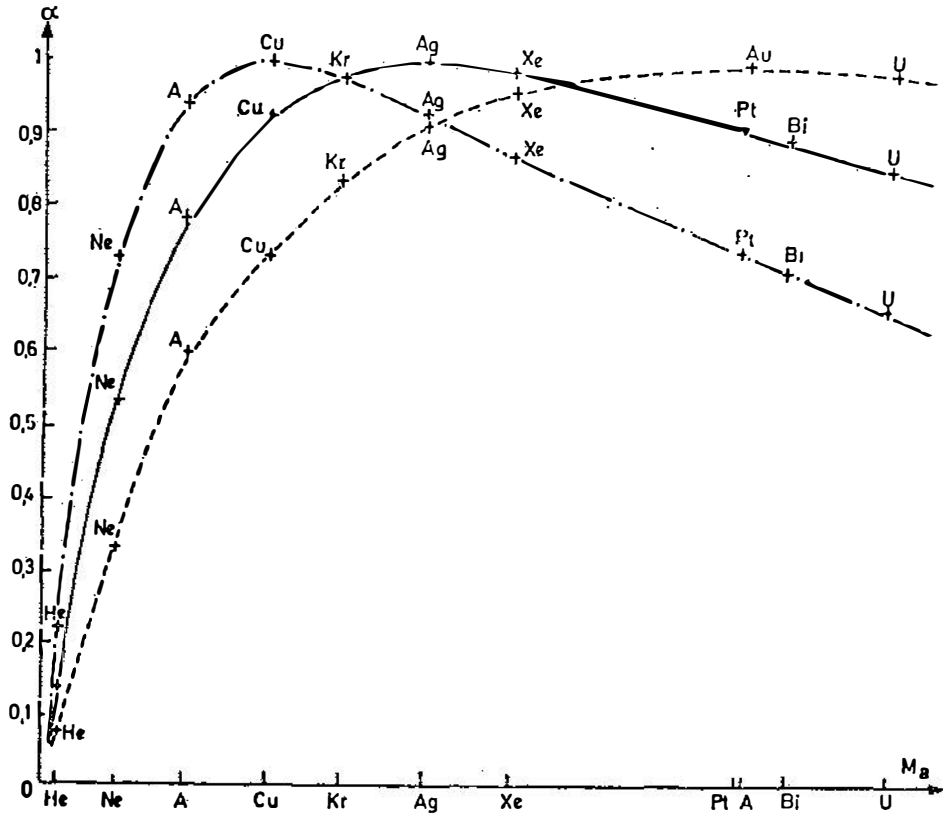


1) Orientations for which the penetration of the incoming ion is very high: on these grains the damage is distributed deep inside the crystal and is largely spread. The local concentration of defects is thus low which means a small probability of cluster formation during their migration. Without cluster formation no starting of the mechanism of relief topography is possible and the surface remains smooth. In our experimental conditions the exact  $\langle 110 \rangle$  pole has this behaviour.

2) Orientations for which the penetration is very poor: the damage lies just under the surface and is densely distributed. On the other hand the sputtering yield is high and the surface regresses thus quickly. Here the migration of the defects into clusters cannot take place before the surface reaches their level. On these grains the instantaneous removal of the disturbed layer prevents the mechanism to start and the surface will remain unattacked if it was clean before the bombardment. Most grains or crystal orientations of high  $hkl$  indices behave in such a way.

For the two previous type of grains, all sorts of cones, spikes, craters and pits will develop on the surface, if this was not clean or well polished before the bombardment.

3) For the grains of medium penetration the surface regresses at such a rate that it is possible for the defects (if their concentration is high enough) to form clusters during their migration, before the surface reaches the level of the perturbed layer. Here the previous mechanism can start and relief topography will be formed on grains of low  $hkl$  indices as for example the  $\langle 100 \rangle$  and the  $\langle 111 \rangle$  grains.



To determine which grains behave in which way during different experiments, one has to know the energy of the incoming ions, their mass, the mass of the target atoms, as well as the target temperature and dosis. For example, an increase of the energy of the incoming ions will give rise to a greater penetration and will thus cause a shift of the crystal orientations of the behaviour 2) to the behaviour 1). Other grains will thus have to be taken into account for the formation of relief topography.

The masses of both target atoms and incident ions, have an influence on the same aspect by the intermediate of the energy transfer coefficient  $\alpha$ .

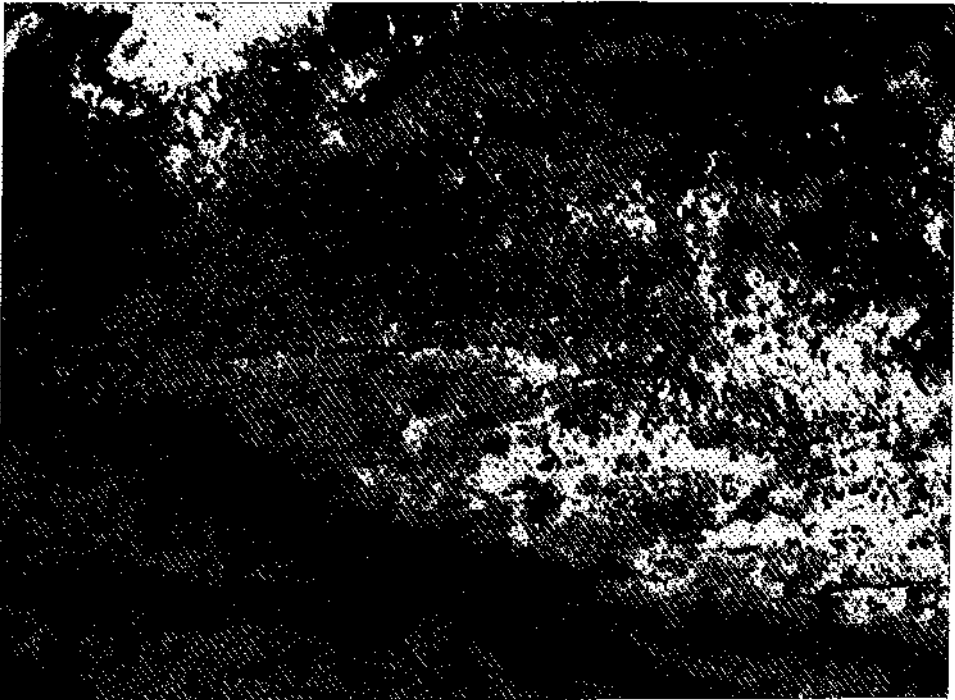


Fig. 1 Transmission electron micrograph of a Cu-foil after a 5 keV  $A^+$  ion bombardment (dosis:  $10^{13}$  ions/s  $cm^2 \times 125s$ ). Pointdefects and clusters induced by the ion bombardment are visible. Grain  $\langle 110 \rangle$ .

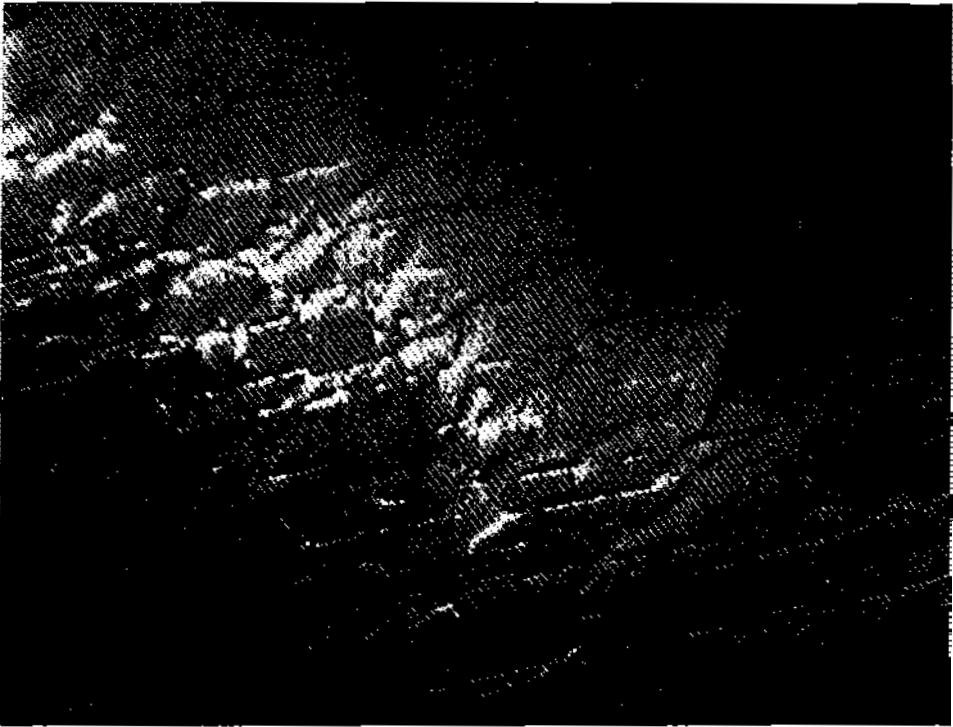


Fig. 2 Cu bombarded with 5 keV  $A^{+}$  ions, at a dose of  $10^{16}$  ions/cm<sup>2</sup>. When the loops, grown out of the clusters, are cutten by the surface, open and interact to form long dislocation segments under the surface (black and white contrast).

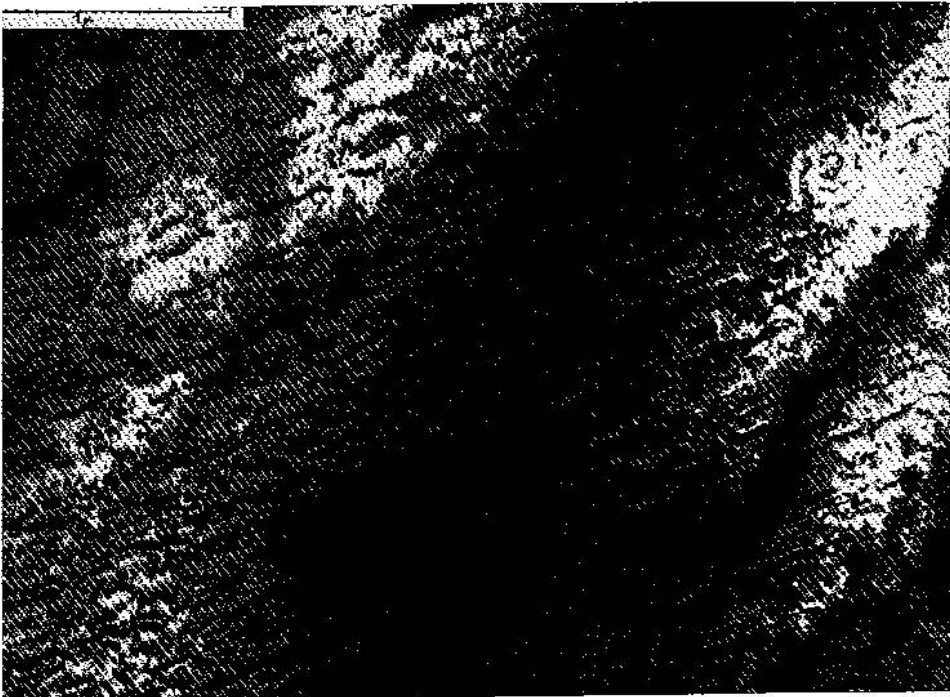


Fig. 3 Transmission electron micrograph of a Cu-foil bombarded with 5 keV  $A^+$  ions (dose of  $10^{13}$  ions/s  $cm^2 \times 30$  s). Alignment of opened loops to form long dislocation segments along the  $\langle 110 \rangle$  directions ( $\langle 211 \rangle$  grain). Burgers vector of the dislocations is  $\langle 022 \rangle$ .

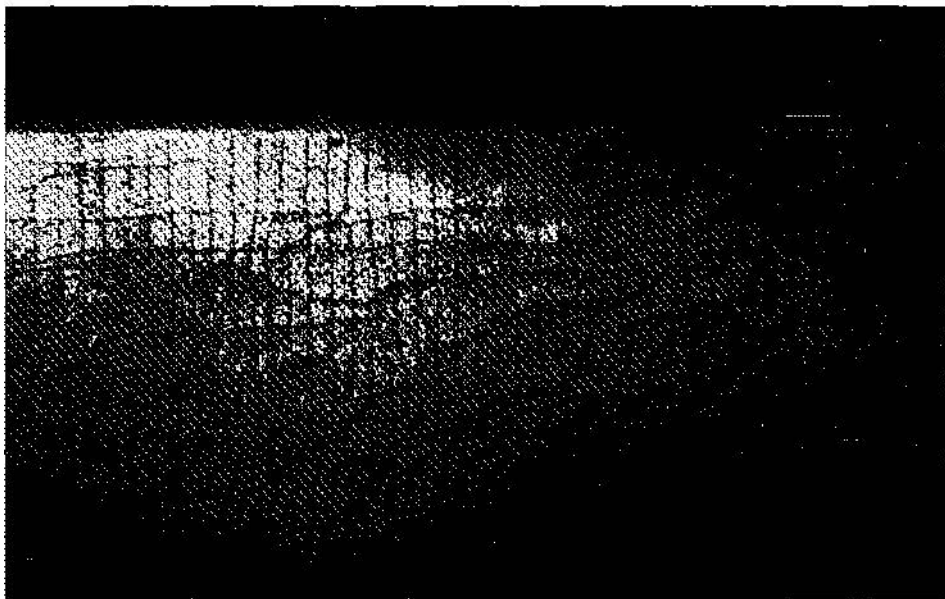


Fig. 4 Cu bombarded with 5 keV A<sup>+</sup> ions, at a dose of 10<sup>16</sup> ions/cm<sup>2</sup>. The dislocations extend over the whole width of the grain. A second system of dislocations is visible, less regular and more looking like stress dislocations. They are probably created to release the stress in the damaged crystal.

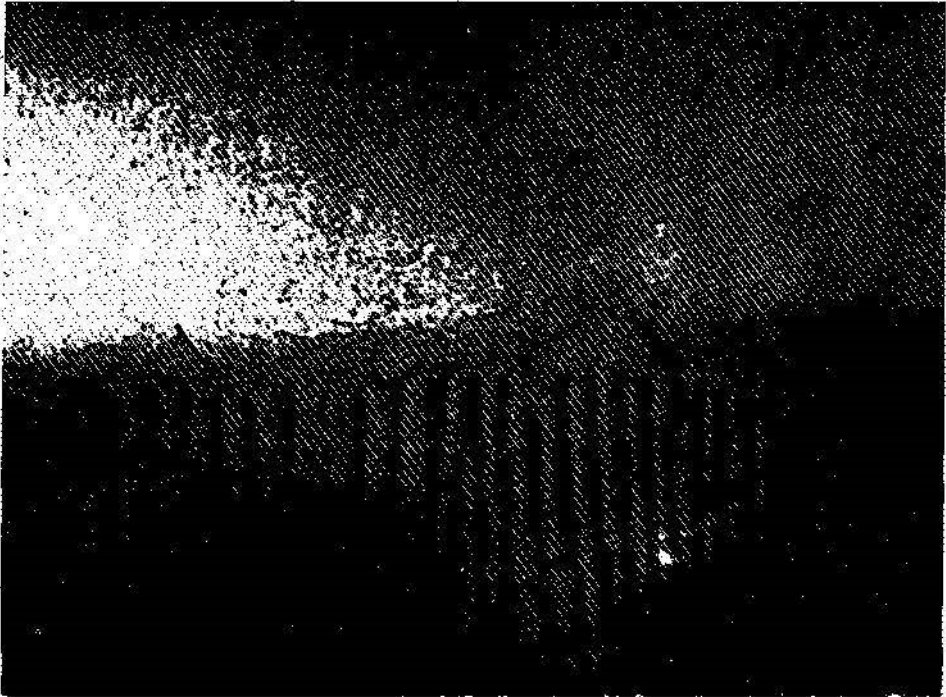


Fig. 5 Transmission electron micrograph of a Cu-foil irradiated with  $5 \text{ keV A}^+$  ions at a dose of  $10^{13} \text{ ions/s cm}^2 \times 360 \text{ s}$ . Dislocations lying very near the foil surface induce the formation of small grooves by a local increase of the sputtering yield.

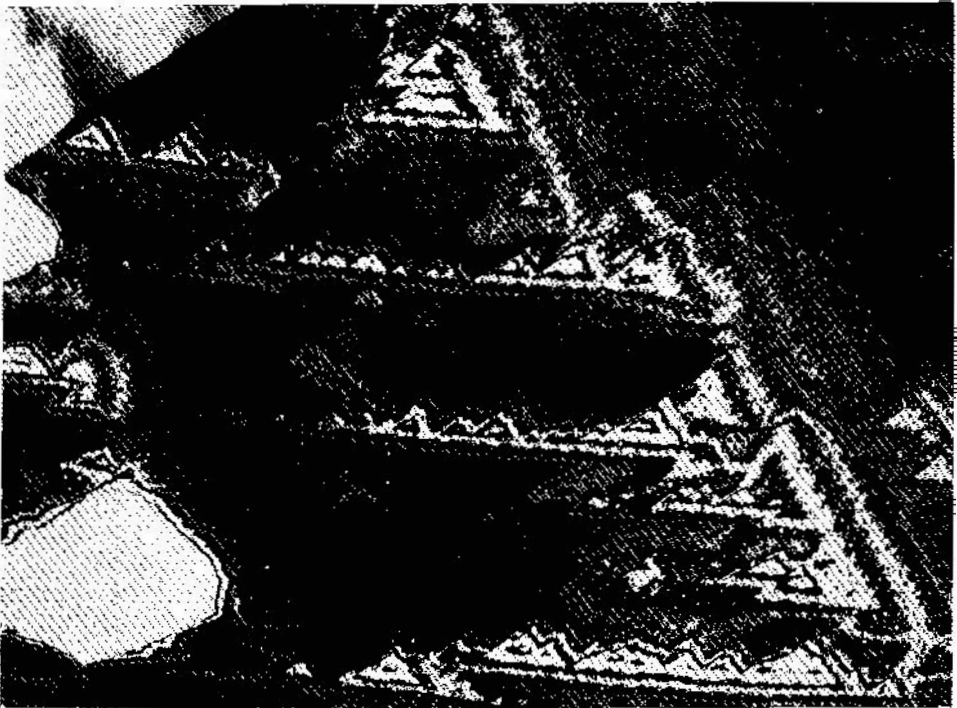


Fig. 6 Cu-foil bombarded with 5 keV  $A^+$  ions at a dose of  $10^{13}$  ions/s  $cm^2 \times 500$  s. On the  $\langle 111 \rangle$  grains, the intersection of three systems of dislocations, each along a  $\langle 112 \rangle$  direction originates a relief structure of triangular craters.

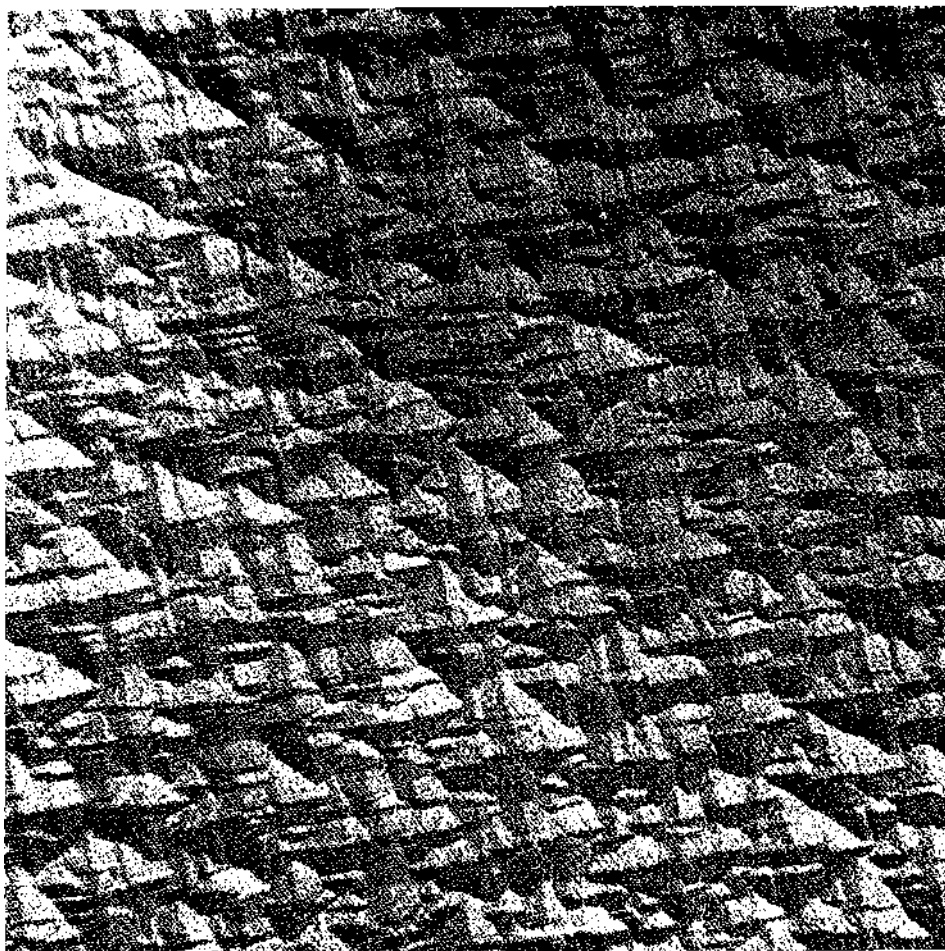


Fig. 7 Replica electron micrograph of a  $\langle 100 \rangle$  grain of bulk Cu bombarded by 5 keV  $A^+$  ions. The relief structure formed by the ion irradiation on this grain is the result of the intersection of two systems of roofs, each aligned along the intersection of the  $(110)$  planes with the foil surface, i. e. along the  $\langle 110 \rangle$  directions. The resulting aspect is one of square-shaped craters.

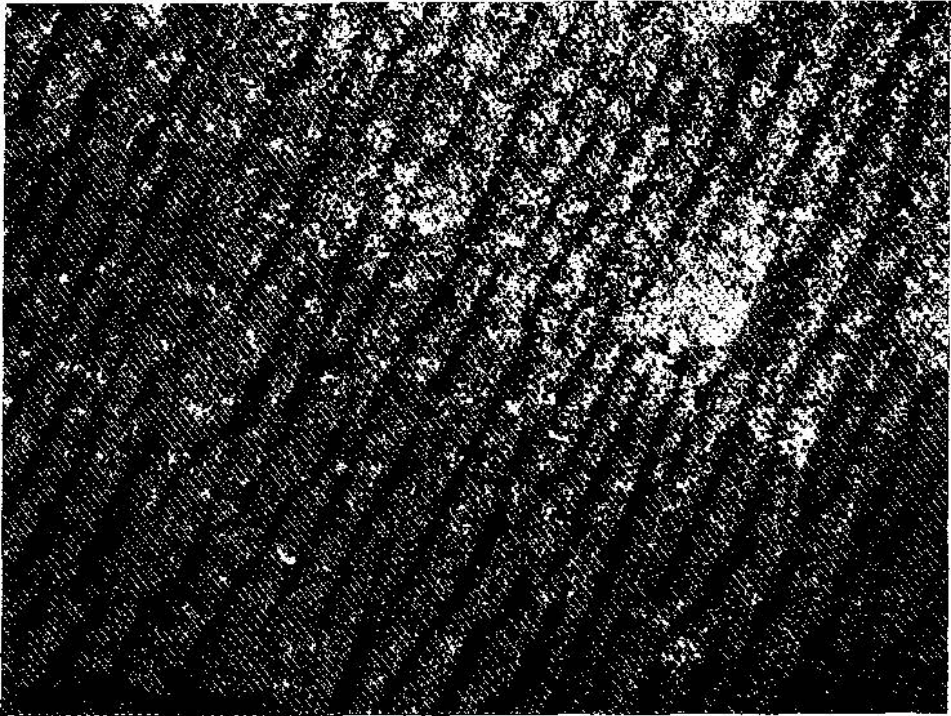


Fig. 8 Transmission electron micrograph of a Cu-foil irradiated with 5 keV  $A^+$  ions at a dose of  $10^{13}$  ions/s  $cm^2 \times 500$  s. A relief structure is appearing on the ion bombarded surface of a  $\langle 110 \rangle$  grain of the foil, the roofs are aligned along the  $\langle 100 \rangle$  direction.



Fig. 9. Cu thin foil bombarded with 5 keV  $A^+$  ions at a dose of  $10^{16}$  ions/cm<sup>2</sup>. Apart of the dislocation segments due to the opening of the loops, another network of dislocation lines is visible, not showing the black and white contrast. These lie thus deeper under the surface and belong to a system of misfit dislocations.



A higher dose as well as a higher target temperature will favour the cluster formation either by increase of the defect concentration, either by increase of their mobility. A shift of the 1) and 2) behaviour towards the 3) behaviour is expected, more grains will be susceptible to develop a relief structure on their surface. The aspect of the „milky appearance“ zone on bombarded mono-crystals (normal incidence) will thus vary with all these parameters.

During the ion bombardment of crystals some other perturbations of the material take place. For certain dose conditions, there exists at a higher depth under the surface a concentration of induced gas atoms and point defects such that the lattice is distorted with respect to the adjacent original matrix. At one or at both junctions with the normal lattice, misfit dislocations will appear (Fig. 9). These dislocation network does not present the black and white contrast observed for the damage induced dislocations. The observed dislocations lie thus deeper under the surface; this corresponds to the fact that the incoming ions generally come to rest behind their collision cascade<sup>10)</sup> and at such a depth the concentration of point defects is not high enough to form clusters.

During the going on of the bombardment, the concentration of the gas atoms increases until finally gas bubbles are formed by coalescence of these after diffusion. At this moment we suppose the misfit dislocations to disappear.

A third system of dislocations is observed in the bombarded thin foils. These dislocations find their origin in the release of the stresses induced in the foil by the previous two systems. This third system is mainly perpendicular to the damage induced network (Fig. 4).

Neither the second system nor the third one seems to have any influence on the formation of the relief structure.

### References

- 1) L. Francken, A. Art and O. Goche, *Phil. Mag.* **15** (1967), 673; N. Hermanne and A. Art, accepted for publication in *Radiation Effects* (1970); N. Hermanne, *mémoire U. L. B* (1969).
- 2) cfr. G. Garter, and J. C. Colligon: *Ion bombardment of Solids*, Heinemann educat. books (1968); D. J. Mazey, R. S. Nelson and P. A. Tackery, *Journ. Mater. Sciences*, **3** (1968) 26.
- 3) G. Carter and J. S. Colligon: *Ion bombardment of Solids*, Heinemann educat. books (1968).
- 4) D. J. Mazey and R. S. Barnes, *VI. Int. Congres for E. M.*, Kyoto (1966); D. M. Maher, and B. L. Eyre, *Phil. Mag.* **17** (1968) 1; D. J. Mazey and R. S. Barnes, *Phil. Mag.* **17** (1968) 387.
- 5) H. Diepers and J. Diehl, *Phys. Stat. Sol.* **16** (1966) 109; K. L. Merkle, *Phys. Stat. Sol.* **18** (1966) 173; P. Sigmund, G. P. Scheidler and G. Roth: *Conf. Sol. State Res. with Accelerators*, N. Y. (1967); D. J. Mazey, R. S. Nelson and R. S. Barnes, *Phil. Mag.* **17** (1968) 1145; L. E. Thomas, T. Schober and R. W. Balluffi, *Rad. Eff.* **1** (1969) 257.
- 6) P. Bowden and D. G. Brandon; *Phil. Mag.* **8** (1963) 935;
- 7) S. Amelinckx, private communication; Y. Quéré: *V. Int. Summ. Sch. Symp. Phys. Ion. Gases*, Herceg-Novi (1970);

- 8) A. D. G. Stewart and M. W. Thompson, *J. of Mater. Science* 4 (1969) 56;
- 9) B. Navinšek, *Eur. E. M. Conf.*, Prague (1964);
- 10) P. Sigmund and J. Sanders, *Conf. Applic. Ion beams to S. Cond. Techn.*, Grenoble (1969).

### 2.16 Observation by E. M. of dislocations networks generated during $A^+$ ion bombardment of thin copper foils

A. ART and N. HERMANNE, *Physique des Surfaces, Faculté des Sciences, Université libre de Bruxelles, Brussels, Belgium*

### 2.17 Power-law potentials deduced from the ion ranges in solids

T. JOKIĆ and R. JANEV, *Institute of Nuclear Sciences „Boris Kidrič“, Beograd, Yugoslavia*

#### *Abstract*

A semiempirical method is proposed to deduce an inverse power-law potential from the experimental data on ion ranges in solids in the energy region 20—70 keV.

Using the usual matching procedure and the experimental values for the penetration depths we derived the parameters of the power-law potentials for the Kr-Al, Cs-Al, Xe-Ni, Xe-Mo and Xe-Cu pairs. Comparing the obtained potentials and the Bohr and Thomas-Fermi ones, one can conclude that this method gives a representation of the interatomic potentials in this energetic region, as good as the Bohr or Thomas-Fermi potentials.

### 2.18 The quantum state of hydrogen atoms reflected at a metallic surface

M. KAJZER and Z. ŠTERNBERG, *Institute „Ruđer Bošković“, Zagreb, Yugoslavia*

### 2.19 Secondary electron emission and glow-to-arc transition in discharges with electrolytes as cathode

Z. ŠTERNBERG, *Institute „Ruđer Bošković“, Zagreb, Yugoslavia*